First-Principles Calculations of Pyridines: From Monomer to Polymer

ARTICLE *in* THE JOURNAL OF PHYSICAL CHEMISTRY A · NOVEMBER 1999

Impact Factor: 2.69 · DOI: 10.1021/jp992204b

4 AUTHORS, INCLUDING:

Bernardo Retamal
Hexcel Corporation
11 PUBLICATIONS **245** CITATIONS
SEE PROFILE

Andy Monkman
Durham University
416 PUBLICATIONS **9,817** CITATIONS
SEE PROFILE

Michael Springborg
Universität des Saarlandes
266 PUBLICATIONS **2,741** CITATIONS
SEE PROFILE

First-Principles Calculations of Pyridines: From Monomer to Polymer

Mariana E. Vaschetto*

MSI, 230/250 The Quorum, Barnwell Road, CB5 8SX Cambridge, U.K.

Bernardo A. Retamal, and Andrew P. Monkman

OEM, Department of Physics, University of Durham, DH1 3LE Durham, U.K.

Michael Springborg

Faculty of Chemistry, University of Konstanz, Fach M722, D-78457 Konstanz, Germany

Received: June 29, 1999; In Final Form: August 25, 1999

The structural and electronic properties of pyridine, its oligomers, and polypyridine (PPY) as obtained with density functional methods are presented in this work. Among the different exchange-correlation functionals used, B3LYP gives good structural results, whereas B3P88 predicts more accurately the electronic properties. The calculated first excitation energies of pyridine systems are in good agreement with experimental data. The coupling between the monomers in forming oligomers influences the structural and electronic properties of the system significantly. The trans head-to-head dimer is found to be the most stable form and the only one having a planar geometry. The introduction of a head-to-head or tail-to-tail coupling in order to break the regioregularity of a tetramer changes the frontier orbitals and the total energy of the system. The inclusion of a head-to-head coupling in the central units of a tetramer leads to a global stabilization of the system and lowers the HOMO, producing an increase in the first electronic excitation energy. Finally, the electronic properties of infinite PPY are obtained by extrapolations from those of finite oligomers. The calculated ionization potential, electronic affinity, and $(\pi-\pi)^1$ transition are 6.3, 3.4, and 2.9 eV, respectively, in excellent agreement with previous experimental reports. Furthermore, the band structures and density of states of PPY are calculated using a DFT-LMTO method. The calculated density of states is in good qualitative and quantitative agreement with experimental UPS spectrum for this system.

1. Introduction

Since the first report of electroluminiscence (EL) of poly(*p*-phenylenevinylene) (PPV) in 1990[1] a lot of research has been carried out in order to produce polymers that emit in the visible spectrum with low applied voltage and with high quantum yield.[2−4] Particularly difficult to obtain are polymers that luminesce with blue wavelengths. However, based on previous knowledge about pyridine and bipyridines, scientists have synthesized poly(2,5-pyridiyl) (commonly known as polypyridine, PPY), which luminesces in the blue region of the spectrum.[5−8] This polymer has opened a new perspective in the organic electroluminiscent materials field. Rigorously, to the best of our knowledge, the synthesized polymer PPY is not a totally regioregular structure, but a random coupled one that has been named by use poly(2,5-pyridiyl). Consequently, from now on, the experimental results discussed on PPY will instead correspond to the random coupled poly(pyridine).

For decades, many theoretical and experimental studies of the electronic transitions of pyridine (NC_5H_5) and pyridine-based systems have been carried out.[9−17] In fact, pyridine is a very important heteroaromatic molecule. Its $\pi-\pi^*$ part of the optical spectrum resembles the spectrum of benzene. Additionally, in the low-energy region of the spectrum, further $n-\pi^*$ transitions can be identified.[15] However, the analysis of the spectra is quite complex, and the assignment of the weak $n-\pi^*$ transitions remains controversial.[14] Although pyridine and its derivatives are well-known systems, several questions remain unsolved for the related larger oligomeric or polymeric systems. Particularly interesting is understanding how the structural properties of these systems influence the electronic properties of the conjugated systems. The understanding of the electronic properties of these materials is essential in order to design new systems with specific emission properties that can be used in light-emitting devices (LEDs).

PPY is analogous to the well-known poly(*p*-phenylene) (PPP). However, PPP possesses both charge conjugation and C_{2v} spatial symmetry, whereas in PPY these symmetries are broken. Furthermore, the inclusion of a nitrogen heteroatom in the pyridine-based systems leads to the introduction of nonbonding (n) orbitals (from the nitrogen lone pair) into the electronic structure.[8,18−21] Furthermore, PPY has a processability advantage over PPP as it is soluble in formic acid.[5,4]

The properties of PPY may vary depending on the kind of coupling between the monomers. Experimental controlling of this coupling seems to be a very difficult task[5,8,9,21] so that only little is known experimentally about how the structure of the system affects the final emission spectrum. Alternatively, to study this problem theoretically, it is necessary first to determine the minimum-energy structure and then to calculate its associated electronic properties. Theoretical methods based on density functional theory (DFT)[22,23] have proven to be very accurate for predicting molecular[24] and polymer properties[25] and are therefore appropriate in the present context.

Polymer properties can be estimated in two ways. The first one involves the analysis of the evolution of the structural and

* Corresponding author. E-mail: mariana@msi-eu.com. Fax: +44 1223 413 301.

10.1021/jp992204b CCC: $18.00
Published on Web 11/20/1999

electronic properties with the length of the chain whereby the polymer properties are obtained from an extrapolation to an oligomer having an infinite number of mers.[18] The second one is more elaborated and amounts to consideration of the infinite periodicity in the calculation.[25]

The excitation energies as well as the photoelectron spectra of pyridine and some smaller oligopyridines have been studied previously. Although, calculations of the excitation energies of the pyridine monomer have been performed using highly sophisticated methods (SAC-CI,[13] EOM-CC,[17] CASSCF, and CASPT2[26]), these methods become computationally too demanding when studying oligopyridines or polypyridines.[26]

In this work, we will use DFT methods to calculate structural and electronic properties of pyridine, oligopyridines, and polypyridine. Rigorously, the density functional methods can be applied to calculate the total energy of the ground state, for example, as a function of structure. The orbitals (Kohn−Sham orbitals[27]) are not electronic orbitals, but mathematical arrangements and their eigenvalues are not directly related to the electronic excitation energies. Nevertheless, it is often a good approximation to neglect these formal inconsistencies and consider them as electronic orbitals as they are in the HF framework.[25] The basal singlet (S_0) and the lowest triplet state (T) of PPY have different symmetries; therefore, they can be studied using DFT method.[25]

Results introduced in this work are divided into two main parts; the first is a systematic analysis of the structures and orbitals of pyridine and oligopyridines obtained using different DFT methods. We will show how the coupling between the monomers influences the structural and electronic properties of large oligomers. In the second part of this work, we will apply the "DFT−LMTO−full potential for helical polymers" method[23] to calculate the band structures and density of states for infinite, periodic polypyridine, and we will compare our results with the experimental photoelectron spectra. Finally, we conclude in the last section.

2. Computational Methods

The geometry of pyridine was completely optimized using the DFT schemes described below. In general, no geometrical constraints were imposed when determining the minimum-energy structure of pyridine and its derivatives unless it is indicated.

We have considered various combinations of exchange-correlation functionals. The exchange functionals used are Becke 88 (B)[28] and the Becke three-parameter hybrid (B3),[29] whereas the correlation functionals used are Lee−Yang−Parr (LYP),[30] Perdew (P86),[31] and Perdew and Wang (PW91).[32] B3LYP indicates that Becke's three-parameter hybrid functional is used in combination with the LYP correlation functional, etc. This functional can be expressed as

$$AE_x^{\text{Slater}} + (1-A)E_x^{\text{HF}} + BE_x^{\text{Becke}} + CE_c^{\text{LYP}} + E_c^{\text{VWN}}$$

B3P86 and B3PW91 are defined analogously and differ only in the use of the respective correlation functional E_c . The values of *A*, *B*, and *C* are 0.80, 0.72, and 0.81 as determined by Becke. The main difference compared with other exchange functionals lies in the incorporation of the exact single-determinantal exchange with a weight of 20%.

The calculations for pyridine and the oligopyridines were carried out using a 6-31G* basis set. The "fine grid" option was used to avoid numerical inaccuracies in the energy calculations. For the ground state, no spin-polarization was allowed. The calculations for the triplet structures were carried out using the 6-31G basis set and allowing a spin polarization. All these calculations were performed using the Gaussian94 package[33] contained in the **Cerius^{2}3.8** environment.[34]

The computational method used to study the infinite, periodic PPY has been described in detail elsewhere[24,26] and shall therefore only briefly be described here. The Kohn−Sham single-particle equations[27]

$$\hat{H}_{\text{KS}}\psi_i(r) = \left[-\frac{h^2}{2m}\nabla^2 + V_{\text{eff}}(r)\right]\psi_i(r) + \epsilon_i\psi_i(r) \qquad (1)$$

are solved by expanding ψ_i in a basis of LMTOs which have the form

$$h_l^{(l)}(\kappa|r-\mathbf{R}_k|)Y_L(r-\mathbf{R}_k) \qquad (2)$$

in the so-called interstitial region (outside all atom-centered, nonoverlapping, so-called muffin-tin spheres). Inside the spheres this function is augmented continuously and differentiable with numerical functions obtained from eq 1 by replacing $V_{\text{eff}}(\mathbf{r})$ by its spherically symmetric part. In eq 2, $L \equiv (l,m)$ describes the angular dependence, $\mathbf{R}_k$ is the position of the *k*th atom, κ is a purely imaginary number whose absolute value is a decay constant, and $h_l^{(1)}$ is a spherical Hankel function. It should be pointed out that the full potential is used in the calculation and not only its muffin-tin part. For the exchange-correlation part of $V_{\text{eff}}(\mathbf{r})$ we used the local approximation of von Barth and Hedin.[35]

The method has been specifically designed for studies on infinite and periodic polymers. The periodicity is used in constructing Bloch waves from equivalent basis functions of different unit cells, i.e., from the *j*th basis function of the *n*th unit cell χ_{jn}, the Bloch waves are defined as

$$\chi_j^k = \lim_{N\to\infty}\frac{1}{\sqrt{2N+1}}\sum_{n=-N}^{N}\chi_{jn}e^{ikn\tau} \qquad (3)$$

being *j* a compound index that describes the site where the basis function are centered and its angular dependence as well as any other dependence that distinguishes the basis functions.

Finally, the quasiunidimensional system, periodic in one dimension, has been obtained by combined symmetry operation, a translation, and a rotation. For polymers, which are infinite, periodic, helical, with straight polymer axis, and isolated it is possible to make use of the symmetry in defining symmetry-adapted Bloch-waves of the atom-centered orbitals. Finally, we should mention the planar geometry used in order to study polymers in our case is a special case of helical geometry. For more details the reader is referred to refs 21 and 23.

3. Results and Discussion

A. Pyridine. During the last 4 decades many studies have been devoted to azabenzene compounds.[12−17,36−40] Pyridine is the simplest and most representative molecule of this family. The pioneering works from Clementi[10] and El Sayed et al.[8,9] in the 1960s established the starting point for the current highly sophisticated calculations carried on by Kitao and Nakatsuji,[13] Ross et al.,[26] Del Bene et al.,[17] Ågren et al.,[14] etc. This body of works provides the framework needed to compare the accuracy of the results achieved by using DFT methods that will be presented in this work.

Table 1 shows the structural parameters of pyridine obtained using different exchange-correlation functionals. In this particular study, symmetry constraints have been used, whereby pyridine was assumed to be planar and having a C_{2v} symmetry.

TABLE 1: Structural Parameters of Pyridine (for Details See Figure 1)[a]

	B3LYP	B3P86	B3PW91	BLYP	BP86	BPW91	exptl[40]
r_1	1.3391	1.3354	1.3365	1.3526	1.3489	1.3490	1.3401
r_2	1.3959	1.3927	1.3941	1.4061	1.4045	1.4044	1.3945
r_3	1.3942	1.3912	1.3925	1.4045	1.4026	1.4026	1.3944
r_4	1.0887	1.0887	1.0894	1.0938	1.0986	1.0987	1.0843
r_5	1.0856	1.0856	1.0863	1.0967	1.0954	1.0954	1.0805
r_6	1.0863	1.0865	1.0872	1.0942	1.0960	1.0960	1.0773
α_1	117.09	117.03	117.03	116.67	116.66	116.64	116.83
α_2	123.76	123.83	123.84	123.94	124.02	124.02	123.90
α_3	118.42	118.38	118.37	118.46	118.39	118.41	118.53
α_4	118.54	118.55	118.55	118.52	118.52	118.51	118.33

[a] All the distances are in angstroms and angles in degrees.

TABLE 2: Pyridine Orbital Energies (in eV)

	B3LYP	B3P86[a]	exptl[36]
13a1	4.20	31.21	
4b1	3.99	0.71	
8b2	3.74	0.52	
12a1	2.53	−0.01	
2a2	−0.26	−1.26	
3b1	−0.61	−1.62	
11a1 (n)	**−6.88**	**−7.76**	**−9.60**
1a2(π)	**−7.11**	**−8.01**	**−9.75**
2b1(π)	**−7.24**	**−8.69**	**−10.51**
7b2	**−7.78**	**−10.71**	**−12.61**
1b1(π)	**−9.90**	**−11.64**	**−13.1**
10a1	**−10.73**	**−11.81**	**−13.8**
6b2	**−10.98**	**−12.47**	**−14.5**
9a1	**−11.66**	**−13.64**	**−15.6**

[a] Structure optimized using B3LYP.

Among the different types of DFT variants, B3LYP and the closely related B3P86 and B3PW91 approaches lead to the best structural results. The hybrid methods are not superior to the gradient correct ones when calculating angles. Furthermore, it has been found that all functionals containing the gradient-corrected exchange functional (Becke 88) consistently produces bond lengths between atoms heavier than hydrogen (i.e., C, N, etc.) which are too long by about 0.01−0.02 Å.[25] Bond lengths are of extreme importance on conjugated systems since the electronic properties are very sensible to any bond length alternation change. The inclusion of a fraction of single-determinantal exchange in the hybrid methods within Becke's three-parameters exchange functionals gives better agreement with the experimentally determined bond lengths. One possible explanation of this may be related to the fact that the inclusion of some exact single-determinantal exchange reduces the spurious self-repulsion more effectively than the way it is handled in gradient-dependent approximations, hence shortening the bond length.

Table 2 shows the Kohn−Sham orbital energies of pyridine calculated using the B3LYP and B3P86 functionals together with the experimental ionization energies. The explicit inclusion of electronic correlation in azacompounds has been found to be crucial when determining the relative position of the *n* and π orbitals. Our DFT results show that although the whole orbital pattern is shifted towards more positive energies compared with the experimental results (by about 1.8 eV), the relative ordering agrees well with the experiment. B3P86 exchange-correlation functional produces smaller absolute errors than its analogues B3LYP. In general, hybrid methods tend to produce eigenvalues with small errors. This is because in the Hartree−Fock calculations the orbital energies are (slightly) too negative and span over a too broad energy range. DFT, on the other hand, gives energies that are too high, but span over a reasonable range. A mixture of the two might therefore give good averages between them. Also, the inclusion of the nonlocal correlation in the P86 expression seems to improve the ability of B3P86 functional in producing more negative Kohn−Sham energies versus B3LYP.

The orbital pattern and the excitation energies of pyridine have been determined experimentally and theoretically with high accuracy. In general, three bands dominate the electronic spectrum of pyridine at ∼4.8, 6.2, and 7.0 eV, which are commonly assigned as $(\pi-\pi^*)^1$ transitions, where the superscript indicates the spin configuration. Also, two further bands attributed to $(n-\pi^*)^1$ transitions are observed at 4.3 and 5.6 eV.[12] The valence nature of the pyridine transitions is confirmed by their persistence in the liquid phase.[37] We have calculated the first $(n-\pi^*)^1$ and $(\pi-\pi^*)^1$ excitation energies as the difference between the orbital energies. This approximation leads to values for this transition of 6.1 and 6.4 eV, respectively. Although, the errors of the calculated excitation energies are large, the trend of this prediction is correct ($n-\pi^* < \pi-\pi^*$). One of the most probable explanations for the deviations can be found in the Kohn−Sham formulation, because here we are considering the Kohn−Sham orbitals as electronic orbitals. The second explanation is related to the fact that the experimental first excitation energy of pyridine actually corresponds to an adiabatic transition, which is smaller than the vertical one. To clarify this point, we have optimized the lowest triplet structure using the spin polarized B3LYP functional and subsequently we have calculated the excitation energies of the $(n-\pi^*)^3$ and $(\pi-\pi^*)^3$ excitations. Thereby, we consider an adiabatic transition and the results obtained are 3.8 eV for the $(n-\pi^*)^3$ and 4.1 eV for the $(\pi-\pi^*)^3$ transition, respectively. These excitation values agree very well with those reported by Innes et al.,[11] who determined the triplet excitation value around 3.7 eV. Therefore, without the vertical transition approximation, the errors of the calculated excitation energies are smaller than 3%. Unfortunately, since the S_1 state corresponds to an excited state, the prediction of its geometry using DF methods is formally not possible, although large progresses have been made in this area in the last years.[41−43]

On the basis of this analysis we have chosen the following scheme of calculation for the pyridine oligomers. First, the structures will be optimized using the B3LYP functional, which provides reliable bond lengths. Then, the optimized structure will be used to calculate the orbital energies using the B3P86 functional.

B. Dimers: Effect of the Coupling. Figure 1 shows a schematic representation of the studied dimers of pyridine. The head-to-tail coupling leads to a dimer, which has no symmetry (2,3′-dipyridine, 2,3′DPY). However, the head-to-head (2,2′dipyridine commonly known as bipyridine, 2,2′DPY**)** and the tail-to-tail (3,3′dipyridine, 3,3′DPY**)** coupling yields to compounds with C_{2v} symmetry (when assuming them to be planar). Furthermore, the conformation of these systems can be either cis (C-2,3′DPY, C-2,2′DPY, or C-3,3′DPY) or trans (T-2,3′DPY**,** T-2,2′DPY, or T-3,3′DPY). In Table 3, we present some selected structural data as well as the total energy of the optimized pyridine dimers. When the dimers are fully optimized, the torsion angle between the rings depends on the configuration of the system. It is clear that the interaction between the nitrogen atoms is stronger in the 2,2′DPY systems, where the torsion angle changes from 180° to 35.4°. These angles are an indication of steric hindrance between the adjacent hydrogens of the two rings as well as the inductive effects introduced by the nitrogen atoms. Since T-2,2′DPY does not have any steric hindrance, this system is planar. Figure 2 shows the change of the total

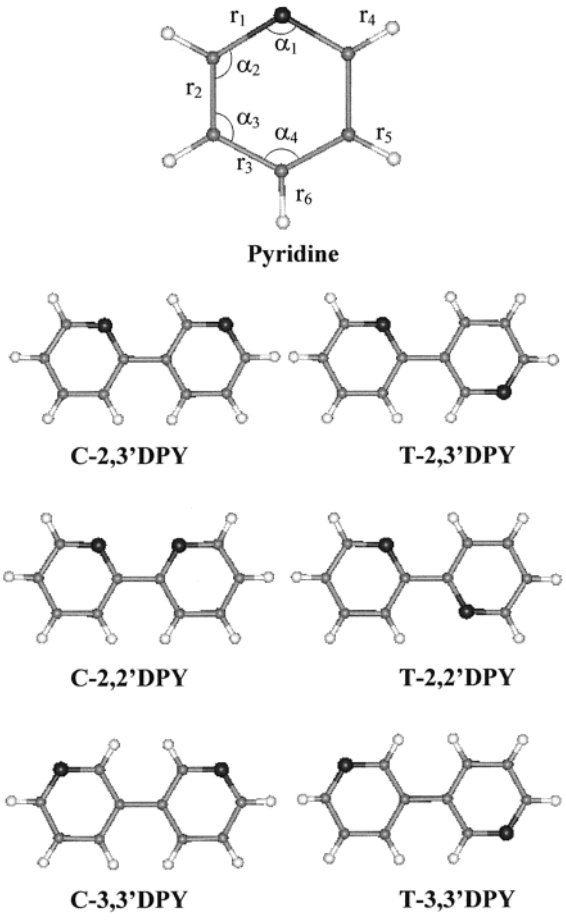

Figure 1. Schematic representation of the pyridine and its dimers.

TABLE 3: Selected Parameters and Total Energy of Optimized Pyridine Dimers (See Figure 1 for Details)

		torsion angle(deg)	interring distance (Å)	total energy (kcal/mol)
2,3′DPy	cis	21.0	1.4854	−310856.185
	trans	162.1	1.4859	−310856.932
2,2′DPy	cis	35.4	1.4940	−310853.479
	trans	180.0	1.4901	−310860.272
3,3′DPy	cis	39.0	1.4802	−310854.282
	trans	141.0	1.4801	−310854.496

energyof the dimers with the torsion angle when going from the cis to trans configuration. The most stable configuration corresponds to the T-2,2′DPY followed by the 2,3′DPY and 3,3′DPY. In fact, depending on the nitrogen position it is possible to go from a very stable trans configuration in the 2,2′DPY case to a 3,3′DPY system where the configuration seems to play a minor role (i.e., essentially the same energy for the cis and the trans conformation). All these calculations have been performed considering the molecule to be in gas phase. However, in the solid state, the behavior will be different. First, dimers are not able to move freely; therefore, it is probable that when the system reaches a conformation that corresponds to a minimum of energy it will stay there, even when it is not the global minimum but a local one. Second, because of the packing restriction in the solid phase, the planar conformation will be preferential, and they will be adopted when the total energy barrier allows it. That is the case of 2,3′DPY, where there are very small variations of its total energy when the torsion angle between rings changes from 160° to 180°.

Considering these differences, it is not surprising that the electronic properties of these systems change when the interring coupling is changed. In a first set of calculations, we forced the dimers to remain planar, allowing the rest of the molecule to be optimized. In this case, the general shape of the orbitals of the six compounds remain very similar. The most important change is observed in the HOMO-1, which is a π-orbital delocalized on both rings. Here, it is important to notice that the HOMO is no longer an n-type orbital, as in the monomer case, but a π-type orbital, and, accordingly, the first electronic excitation will correspond to a $\pi-\pi^*$ one.

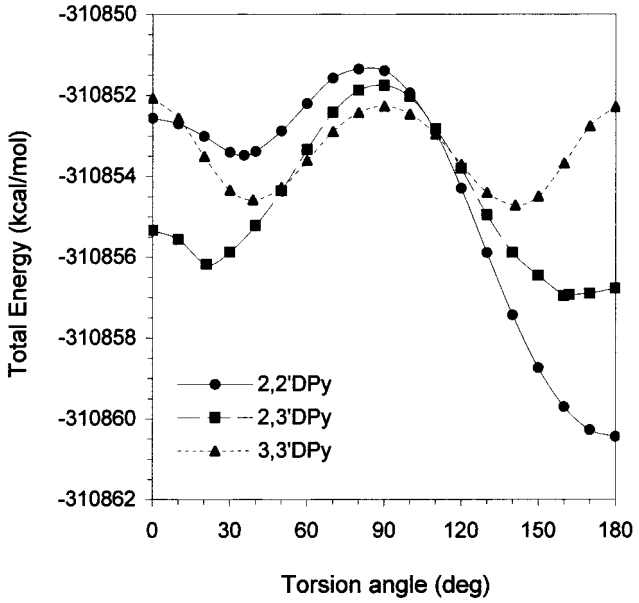

Figure 2. Relative total energy of the different dimers vs the torsion angle between rings.

TABLE 4: Pyridine Dimers Orbital Energies (in eV)

	T-2,2′DPY	T-2,3′DPY	T-3,3′DPY
35	−10.26	−10.46	−10.48
36	−8.71	−8.97	−9.11
37	−8.45	−8.52	−8.53
38	−8.13	−8.19	−8.29
39	−7.81	−7.73	−7.91
40	−7.37	−7.51	−7.51
HOMO	−7.03	−7.15	−7.30
LUMO	−1.99	−2.02	−1.93
43	−1.32	−1.41	−1.47
44	−0.83	−1.05	−1.33
45	0.18	−0.02	−0.39
46	2.33	2.00	2.194
47	2.37	2.56	2.209

The orbital patterns of bipyridine-type systems are strongly affected by the configuration. For example, the planar C-2,2′DPY has a C_{2v} spatial symmetry and the coupling between nitrogen atoms reaches a maximum for C-2,2′DPY. In this case, the occupied n and π orbitals are located very close in energy. Furthermore, the frontier orbitals of 2,2′DPY are destabilized compared to those of 2,3′DPY.

Previously, it has been suggested that the spatial symmetry on the head-to-head or head-to-tail plays only a minor role in the absorption spectrum of the pyridine dimers.[18] These results have been obtained considering the structures as being planar. Here, we find in contrast that the couplings between the monomers play an important role in determining the origin of the transitions, partly due to the different extents of mixing of the n and π orbital according to the conformation and configuration of the pyridine dimers (see Table 4).

C. Tetramers: Random Coupled vs Regioregular Pyridine Tetramers. Figure 3 shows three different structures of tet-

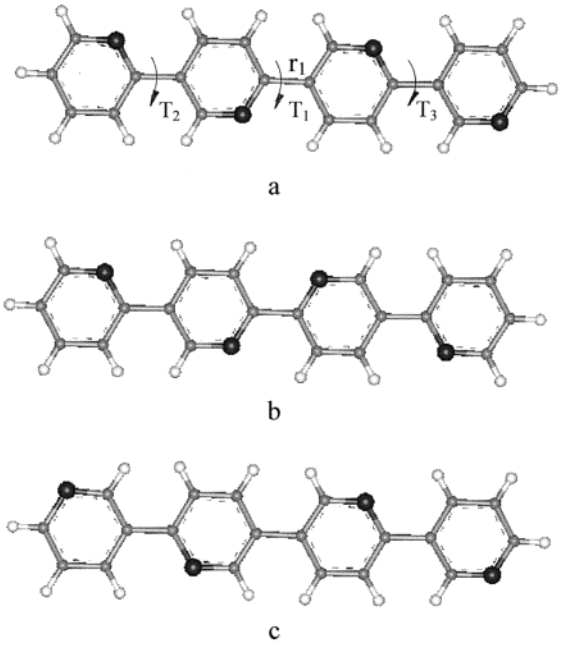

Figure 3. Optimized structures of different pyridine tetramers. T2, T1, T3 are the angles between the planes defined by adjacent rings.

TABLE 5: Selected Structural Parameters of Pyridine Tetramers (see Figure 3 for Details)[a]

	structure **3a**	structure **3b**	structure **3c**
r_1	1.481	1.485	1.476
T_1	164.2	179.7	143.8
T_2	163.5	162.4	162.8
T_3	162.7	162.4	162.8

[a] All the bond lengths are in angstroms and angles in degrees.

ramers optimized using the B3LYP functional. The structures **3b** and **3c** can be considered as representatives of random coupled systems because they contain a head-to-head or a tail-to-tail coupling in the central unit. On the other hand, the structure **3a** is a regioregular system. Some selected structural parameters of these systems are listed in Table 5. They can be easily associated with those of the dimers (i.e., enlargement of the distance between the central rings as well as a reduction of the central torsion angle for the system containing a 2,2′ coupling related to the regioregular tetrapyridine, whereas the opposite effect is observed for the system having a 3,3′ coupling). The most important feature is the change of the torsion angle between pyridines when a head-to-head coupling is present. Finally, the total energy depends on the configuration of the system with the structure **3b** being more stable than the **3a** and **3c** ones (by ~3 and ~6 kcal/mol, respectively).

In addition to these structural variations, changes in the structure will alter the conjugation path of this system producing substantial modifications of the orbital couplings. Table 6 shows the orbital energies of the three structures shown in Figure 3. The structure containing a head-to-head coupling shows a destabilization of the HOMO related to the regioregular structure, whereas the opposite effect is observed for the structure having a tail-to-tail coupling. Depending on the coupling, the HOMO orbital changes up to 0.3 eV, whereas the LUMO varies only about 0.1 eV. This will have direct consequences for the electronic transitions. From these results, one may suggest that, since the periodicity is broken in nonregioregular PPY, the frontier orbitals, which control excitation processes in the UV-vis region will span a broader energy region. The immediate experimental consequence of this fact will be the occurrence of broad excitation peaks. In fact, the PPY excitation spectrum shows poor resolution that could be due to the coupling mechanism, which is not 2,5 but random as was explained above.[7,44]

TABLE 6: Pyridine Tetramers Orbital Energies (in eV)

	structure **3a**	structure **3b**	structure **3c**
75	−8.13	−8.09	−8.24
76	−7.64	−7.81	−8.12
77	−7.59	−7.69	−7.80
78	−7.54	−7.68	−7.64
79	−7.44	−7.50	−7.63
80	−7.26	−7.34	−7.53
HOMO	−6.86	−6.60	−6.91
LUMO	−2.56	−2.56	−2.66
83	−1.75	−1.62	−1.92
84	−1.60	−1.44	−1.61
85	−1.37	−1.35	−1.61
86	−1.35	−1.05	−1.20
87	−1.15	−0.88	−1.18
88	−0.55	−0.35	−0.49
89	0.38	0.79	0.267

D. Electronic Properties of Pyridine Oligomers as a Function of the Chain Length. When going from the monomer to the infinite polymer, the electronic excitations of the system gradually change. The electronic properties of a polymer can be estimated using the empirically well-known linear relationship: $E_{\text{oligomer}(m)} = E_{\text{polymer}} + A/m$, where A is a constant and E is either the total energy, the excitation energy, the ionization potential (IP), or the electronic affinity (EA).[18] Therefore, E_{polymer} can be obtained from the extrapolation of the oligomer properties in the limit $m \rightarrow \infty$ ($1/(m \rightarrow 0)$), with m being the number of monomer units. In our case, pyridine not only changes its electronic properties but also its structural properties when increasing the chain length. In fact, the torsion angle between the rings decreases with the chain length, suggesting that there is a compromise between the electronic delocalization and the steric hindrance between hydrogen atoms of adjacent rings. In fact, from Figure 2 it is clear that the energy difference between the planar (180°) and the most stable T-2,3′DPY is smaller than 0.2 kcal/mol. Such a small barrier can be easily overcome, and the system could remain planar. Thus, for large regioregular pyridine oligomers this energy can be compensated by electronic delocalization. Considering that our calculations have been performed in the gas phase, it is reasonable to consider that in the solid state the regioregular system could be found in a planar state. In conclusion, in long regioregular oligomers the electronic delocalization seems to play a dominant role making the whole system quasiplanar. For instance, pyridine pentamer and hexamers optimized using the B3LYP method show a decrease of the bond length between rings, and simultaneously the whole system becomes more planar. Figure 4 illustrates this effect, here the torsion angle considered is between the two central pyridine rings of the oligomer; also the bond length plotted is the distance between these rings.

The IP and EA of the oligomers display a quasilinear relationship with $1/m$. The predicted IP and EA of the regioregular PPY, obtained from the intercept ($1/(m \rightarrow 0)$), are 6.3 and 3.4 eV (see Figure 5a). These values are in good agreement with the experimental values reported by Miyamae et al., which are 6.3 and 3.5 eV, respectively.[6,45]

The fluorescence properties of pyridine compounds are very important for their photophysical applications. In general, the fluorescence of a compound depends of the relative position of the (n−π^*) transitions compared with the lowest singlet (π−π^*) one. This is because the intersystem crossing between (n−

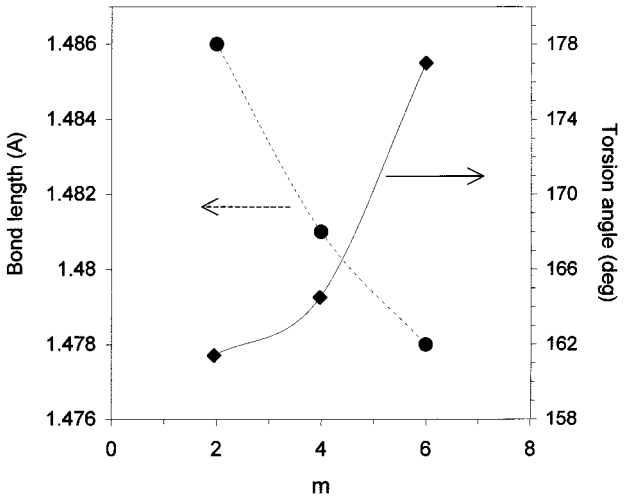

Figure 4. Torsion angle and bond distance between the two central units of oligopyridines as a function of the number of monomeric units.

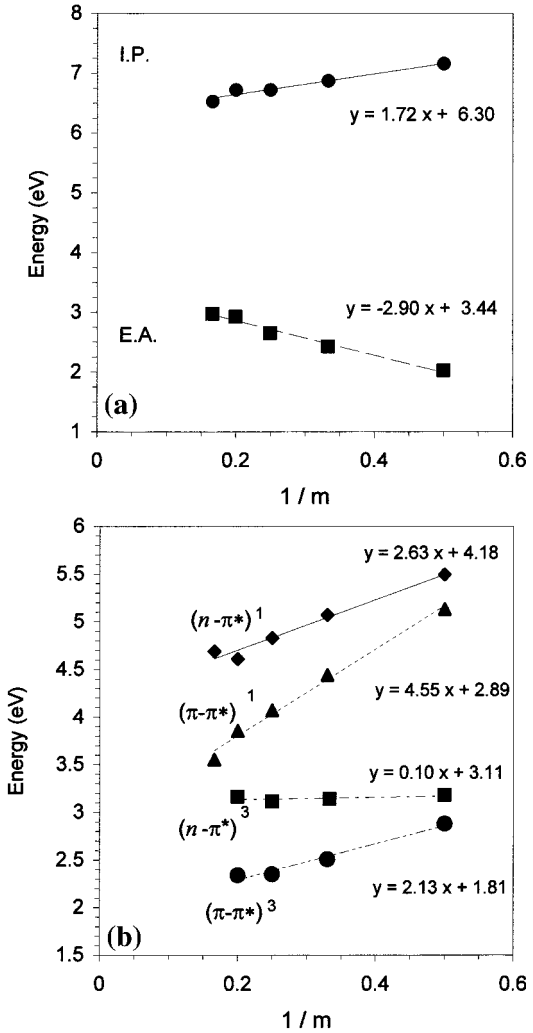

Figure 5. (a) Evolution of the IP and EA with 1/*m*. (b) Evolution of the $(\pi-\pi^*)^1$, $(n-\pi^*)^1$, and $(\pi-\pi^*)^3$ transition energies with 1/*m*.

π^*) and $(\pi-\pi^*)$ is allowed and molecules, for which the $(n-\pi^*)$ transition energy is lower than the $(\pi-\pi^*)$ one, fluoresce only weakly. Figure 5b shows the change of the electronic transitions of the regioregular oligopyridines as a function of 1/*m*. Results obtained using the B3P86 functional show that there is lowering of the electronic transitions when *m* increases. However, the changes of the $(n-\pi^*)^1$ transition are less than in the $(\pi-\pi^*)^1$ due to the more localized nature of the n orbitals. These results are in agreement with those obtained by Blatchford et al.[18] They have calculated the pyridine oligomer transition energies using the semiempirical PM3-CI method. They have predicted, by extrapolating to $m \rightarrow \infty$, values of ~3.1 eV $(\pi-\pi^*)^1$ and of ~3.9 eV $(n\text{-}\pi^*)^1$. However, they have only considered the oligomer systems with head-to-head couplings.

Predictions of the triplet transition are estimated using the same scheme as for the pyridine case. The spin-polarized B3LYP and B3P86 exchange-correlation functionals were employed to calculate the triplet state. Figure 5b shows the calculated $(\pi-\pi^*)^3$ and $(n-\pi^*)^3$ transitions of the different oligomers. The energy of the $(n-\pi^*)^3$ transition does not change significantly as the chain length increases this an indication of the localized nature of the orbitals involved in the excitation process. Although the energy of the $(\pi-\pi^*)^3$ transition changes more substantially with the chain length, this change remains smaller than in the $(\pi-\pi^*)^1$ case. Our results are in good agreement with previous pulse radiolysis experiments which give a first triplet excitation around 2.2 eV for PPY very close to the predicted 1.8 eV.[44,46]

E. Electronic Structure of Regioregular Poly(2,5-pyridiyl) (PPY). Although the results presented above are seen to be accurate, the predictive power of these calculations is obscured by the fact of the relationship linking the oligomer properties and those of the polymer is based on an empirical estimate. Therefore, it is expected that the actual band structures of the infinite system will give more reliable information about the electronic nature of this system. To get these results we have calculated the band structures of PPY using as structural input data the optimized central unit of regioregular pyridine pentamer. Furthermore, to make our calculations computationally less demanding, we have considered the PPY as being planar and having the nitrogen in alternating positions, resulting in a regioregular system.

We have mentioned above that PPY luminesces in the blue region of the visible spectrum. To date, the only conjugated polymers found to emit in this region are poly(alkylfluorenes), PPP, and PPY. Figure 6a shows the band structures of PPY calculated using the "DFT−LMTO−for helical polymers" method described in ref 21. The PPY band structure shows three π bands and three π^* bands. The most remarkable fact is the appearance in the bonding region of a very flat band, which mainly originates from the n lone pair of the nitrogen atoms.[19] This is in reasonable agreement with the orbital pattern of pyridine and pyridine oligomers reported above as well as with results for polycarbonitrile[47] and polypyrrole.[48] From our calculations we can determine an $(n-\pi^*)^1$ transition around 3.16 eV and a $(\pi-\pi^*)^1$ one around 2.53 eV. These values are in reasonably good agreement with those ones determined experimentally, where the $(\pi-\pi^*)^1$ transition is around 2.9 eV. The comparison of these results with those predicted using the combination B3LYP−B3P86 described above shows that both methods are reliable and they are in good agreement with the experiment, although the inclusion of hybrid methods yields smaller error than the "DFT−LMTO−for helical polymers" method. The explanation for this fact may be due to different aspects. Thus, while in the periodic calculations the LDA of von Barth and Hedin is employed, oligomers calculations are performed using the B3P86 exchange correlation functional. Here, HF contributions are included in the exchange functional and the correlation functional is nonlocal. Notice that also the basis sets are different and this may cause some differences. Furthermore, long-range electrostatic potentials may be an

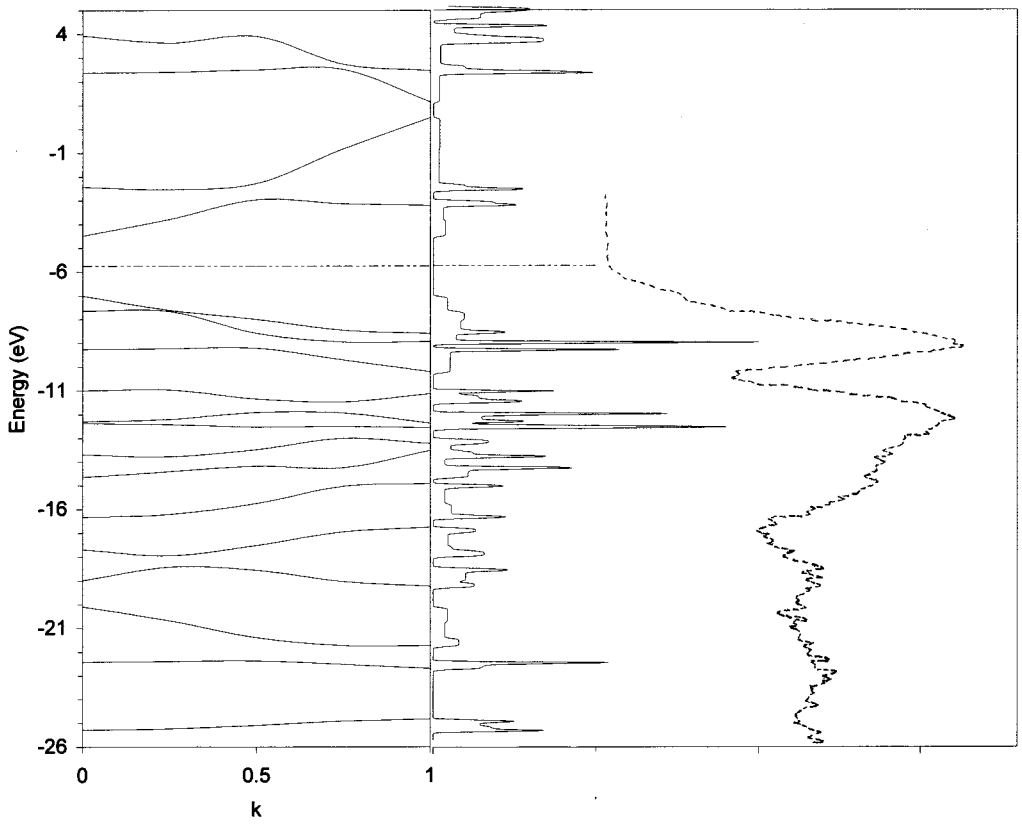

Figure 6. (a) Band structures of regioregular PPY calculated using DFT-LMTO method for helical polymers. (b) Calculated DOS spectrum (solid line) and experimental UPS spectrum (dashed line). The UPS spectrum was taken from ref 6.

additional reason. Since the unit cell is neutral, there will be no long-range $1/r$ potentials, but dipole potentials going as $1/r^2$ may exist. Finally, structural features can contribute to this energy difference.

The calculated density of states (DOS) of PPY is shown in Figure 6b. The experimental UPS spectrum measured by Miyamae et al.[6] is included for comparison. In the experimental UPS spectrum six main features are observed at 7.1, 9.2, 12.4, 15.0, 18.8, and 22.7 eV. Our DOS spectrum gives account of every experimental feature having remarkable good agreement for predicting the main peaks and the valleys of the UPS spectrum. Previous semiempirical calculations show problems in predicting the correct position of the *n*-band. Also, semiempirical calculations of the DOS must be rescaled in order to match the experimental spectrum.[6,18,44]

4. Summary

In this work, we have calculated the structural and electronic properties of finite and infinite oligopyridines using DFT-based methods. The results show a very good agreement with other available theoretical or experimental information. Among the different types of DFT variants, the combination of Becke's hybrid exchange (B3) and the gradient corrected Lee−Yang−Parr (LYP) correlation functional was most accurate in predicting bond lengths. However, the B88 exchange functional gives smaller relative error when calculating the electronic parameters of these systems.

The torsion angle between rings in the pyridine dimers is very dependent on the configuration of the dimers. T-2,2DPY is the only structure to show an energy minimum when it is planar. However, other systems, i.e., T-2,3′DPY, need a very small amount of energy to become planar. Therefore, since our calculations have been performed in the gas phase, we can expect that in the solid phase the systems remain planar. Here, we shall point out that when increasing the number of mers in the chain the torsion angles between rings decreases until they reach a value near to zero for long oligomers. This is because the delocalization energies overcome the steric hindrance between adjacent rings.

DFT methods predict relative positions of the orbitals that are in good agreement with experimental information. Here, the HOMO orbital of pyridine is found to be an n-type orbital, whereas for oligomers the HOMO changes over to a π-type. This difference can be explained in terms of the delocalized nature of the π orbitals, which will lower their energies as their chain length increases. However, the energy of the *n* orbitals remains almost constant as a function of the size of the system. Therefore, the $(\pi-\pi^*)^1$ transition of the polymer is located at a lower energy than the $(n-\pi^*)^1$. This provides an explanation of why monomers (or short oligomers) do not fluoresce (or fluoresce only weakly) compared with the polymer. Another alternative explanation to this fact could be the cooperative spontaneous emission of molecular aggregates or super-radiance. Molecular aggregates are often characterized by ultrafast radiative decays. The classical explanation for this fact is that when a collection of dipoles oscillates in phase, their amplitudes add up coherently to form a large effective dipole. The oscillator strength and consequently the radiative decay are then proportional to the number of dipoles. Thus, the radiative rate is fast, so that fluorescence can compete more effectively with other decay processes.[49−51]

The coupling between the monomers plays a major role in determining the structural and electronic properties of these systems. Also, the random coupling in tetramers may produce a shift of the frontier orbitals. These changes will cause a

broadening of the excitation peaks when studying nonregioregular systems.

By applying an extrapolation from the electronic properties of the finite oligomers, the predicted first electronic transition as well as the IP and EA of PPY show excellent agreement with the experimental values reported by Miyamae et al.[6,45] and Monkman et al.[3] Also, remarkably good agreement between the triplet excitation energies predicted by using DFT methods and the experimental values measured by pulse radiolysis.

Using the DFT method for helical polymers, we have estimated a band gap (related to the first $(\pi-\pi^*)^1$ transition) that is in good agreement with the experimental values (error around 10%) and a remarkably good DOS spectrum, which compares very well with the experimental UPS spectrum of Miyamae et al.[6]

Acknowledgment. This work was supported by EPSRC (U.K.). The authors are thankful for the comments of an anonymous reviewer. Also, we thank Prof. Yamamoto and Dr. Miyamae for the PPY UPS spectrum. Finally, the authors deeply appreciate the support from MSI (Molecular Simulations Ltd.).

References and Notes

(1) Borroughes, J. H.; Bradley, D. D. C.; Brown, A. R.; Marks, R. N.; MacKay, K.; Friend, R. H.; Burn, P. L.; Holmes, A. B. *Nature* **1990**, *347*, 539.

(2) Kraft, A.; Grimsdale, A. C.; Holmes, A. B. *Angew. Chem., Int. Ed. Engl.* **1998**, *37*, 402.

(3) Monkman, A. P.; Halim, M.; Rebourt, H.; Samuel, I. D. W.; Sluch, M.; Horsburgh, L. E. *SPIE* **1997**, *3145*, 208.

(4) Gebler, D. D.; Wang, Y. Z.; Blatchford, J. W.; Jessen, S. W.; Lin, L.-B.; Gustafson, T. L.; Wang, H. L.; Swager, T. M.; MacDiarmid, A. G.; Epstein, A. J. *J. Appl. Phys.* **1995**, *78*, 4264.

(5) Yamamoto, T.; Zhou, Z.-H.; Kinbara, T.; Maruyama, T. *Chem. Lett.* **1990**, 223.

(6) Miyamae, T.; Yoshimura, D.; Ishii, H.; Ouchi, Y.; Seki, K.; Miyazaki, T.; Koike, T.; Yamamoto, T. *J. Chem. Phys.* **1995**, *103*, 2738.

(7) Dailey, S.; Halim, M.; Rebourt, E.; Horsburgh, L. E.; Samuel, I. D. W.; Monkman, A. P. *J. Phys.: Condens. Matter* **1998**, *10*, 5171.

(8) El Sayed, M. F. A.; Kasha, M.; Tanaka, Y. *J. Chem. Phys.* **1961**, *34*, 334.

(9) El Sayed, M. A. *J. Chem. Phys.* **1962**, *36*, 552.

(10) Clementi, E. *J. Chem. Phys.* **1967**, *46*, 4731.

(11) Innes, K. K.; Ross, I. G.; Moomaw, W. R. *J. Mol. Spectrosc.* **1988**, *132*, 492.

(12) Bolovinos, A.; Tsekeris, P.; Philis, J.; Pantos, E.; Andritsopoulos, G. *J. Mol. Spectrosc.* **1984**, *103*, 240.

(13) Kitao, O.; Nakatsuji, H. *J. Chem. Phys.* **1988**, *88*, 4913.

(14) Ågren, H.; Knuts, S.; Mikkelsen, K. V.; Jensen, H. J. Aa. *Chem. Phys.* **1992**, *159*, 211.

(15) Al-Joboury, M. I.; Turner, D. W. *J. Chem Soc.* **1964**, 4434.

(16) Turner, R. E.; Vaida, V.; Molini, C. A.; Berg, J. O.; Parker, D. H. *Chem. Phys.* **1978**, *28*, 47.

(17) Del Bene, J. E.; Watts, J. D.; Bartlett, R. J. *J. Chem. Phys.* **1997**, *106*, 6051.

(18) Blatchford, J. W.; Gustafson, T. L.; Epstein, A. J. *J. Chem. Phys.* **1996**, *105*, 9214.

(19) Vaschetto, M. E.; Monkman, A. P.; Springborg, M. *J. Mol. Struct. (THEOCHEM)* **1999**, *468*, 181.

(20) Gebler, D. D.; Wang, Y. Z.; Blatchford, J. W.; Jessen, S. W.; Lin, L.-B.; Gustafson, T. L.; Wang, H. L.; Swager, T. M.; MacDiarmid, A. G.; Epstein, A. J. *J. Appl. Phys.* **1995**, *78*, 4264.

(21) Magnuson, M.; Yang, L.; Guo, J.-H.; Såthe, C.; Agui, A.; Hordgren, J.; Luo, Y.; Ågren, H.; Johansson, N.; Salaneck, W. R.; Horsburgh, L. E.; Monkman, A. P. *Chem. Phys.* **1998**, *237*, 295.

(22) Hohenberg, P.; Kohn, W. *Phys. Rev. B* **1964**, *136*, 864.

(23) Springborg, M.; Andersen, O. K. *J. Chem. Phys.* **1987**, *87*, 7125.

(24) Vaschetto, M. E.; Retamal, B. A.; Monkman, A. P. *J. Mol. Struct. (THEOCHEM)* **1999**, *468*, 209.

(25) Springborg, M. In *Density-Functional Methods in Chemistry and Materials Science*; Springborg, M., Ed.; John Wiley & Sons: Chichester, 1997.

(26) See, for example: Roos, B. O.; Fülscher, M.; Malmqvist, P.-A.; Merchán, M.; Serrano-Andés, L. In *Quantum Mechanical Electronic Structure Calculations with Chemical Accuracy*; Langhoff, S. R., Ed.; Kluwer Academic Publishers: Dordrecht, 1994; p 357.

(27) Kohn, W.; Sham, L. *Phys. Rev. A* **1965**, *140*, 1133.

(28) Becke, A. D. *Phys. Rev. A* **1988**, *38*, 3098.

(29) The original three-parameter hybrid was suggested in the following: Becke, A. D. *J. Chem. Phys.* **1993**, *98*, 5648. The form implemented in Gaussian packages is slightly modified.

(30) Lee, C.; Yang, W.; Parr, R. G. *Phys Rev. B* **1988**, *37*, 785.

(31) Perdew, J. P. *Phys. Rev. B* **1986**, *33*, 8822.

(32) (a) Perdew, J. P. In *Electronic Properties of Solids '91*; Ziesche, P., Eschrig, H., Eds.; Akademie Verlag: Berlin, 1991. (b) Perdew, J. P.; Wang, Y. *Phys. Rev. B* **1992**, *45*, 13244.

(33) Frisch, M. J.; Trucks, G. W.; Schlegel, H. B.; Gill. P. M. W.; Johnson, B. G.; Robb, M. A.; Cheeseman, J. R.; Keith, T.; Petersson, G. A.; Montgomery, J. A.; Raghavachari, K.; Al-Laham, M. A.; Zakrzewski, V. G.; Ortiz, J. V.; Foresman, J. B.; Cioslowski, J.;. Stefanov, B. B.; Nanayakkara, A.; Challacombe, M.; Peng, C. Y.; Ayala, P. Y.; Chen, W.; Wong, M. W.; Andres, J. L.; Replogle, E. S.; Gomperts, R.; Martin, R. L.; Fox, D. J.; Binkley, J. S.; Defrees, D. J.; Baker, J.; Stewart, J. P.; Head-Gordon, M.; Gonzalez, C.; Pople, J. A. *Gaussian 94*, revision E.2; Gaussian, Inc., Pittsburgh, PA, 1995.

(34) *Cerius*^{2} *3.8 User Guide*; Molecular Simulations Inc.: San Diego, 1998.

(35) von Barth, U.; Hedin, L. *J. Phys. C* **1972**, *5*, 1629.

(36) Kimura, K.; Katsumata, S.; Achiba, Y.; Yamazaki, T.; Iwata, S. In *Handbook of HeI Photoelectron spectra of fundamental organic molecules*; Halsted Press: New York, 1981.

(37) MacRae, R. A.; Williams, M. W.; Arakawa, E. T. *J. Chem. Phys.* **1974**, *61*, 861.

(38) Walker, I. C.; Palmer, M. H.; Hopkirk, A. *Chem. Phys.* **1989**, *141*, 365.

(39) Sabaye Moghaddam, M.; Bawagan, A. D. O.; Tan, K. H.; von Niessen, W. *Chem. Phys.* **1996**, *207*, 19.

(40) Buenker, R. J.; Philips, R. A. *J. Mol. Struct. (THEOCHEM)* **1985**, *123*, 291.

(41) Ziegler, T.; Rauk, A.; Baerends, E. J. *Theor. Chim. Acta* **1977**, *43*, 261.

(42) Bauernschmidtt, R.; Ahlrichs, R. *Chem. Phys. Lett.* **1996**, *256*, 454.

(43) Bauernschmidtt, R.; Ahlrichs, R.; Hennrich, F. H.; Kappes, M. M. *J. Am. Chem. Soc.* **1998**, *120*, 5052.

(44) Hartwell, L. J.; Vaschetto, M. E.; Horsburgh, L. E.; Monkman, A. P. *Synth. Met.* **1999**, *101*, 807.

(45) Miyamae, T.; Yoshimura, D.; Ishii, H.; Ouchi, Y.; Miyazaki, T.; Koike, T.; Yamamoto, T.; Seki, K. *J. Electron. Spectrosc. Relat. Phenom.* **1996**, *78*, 399.

(46) Monkman, A. P.; Horsburgh, L. E.; Hartwell, L. J.; Burrows, H.; Miguel, M. G. Unpublished results.

(47) Springborg, M. *Z. Naturforsch* **1993**, *48a*, 159.

(48) Springborg, M.; Schmidt, K. Unpublished results.

(49) Mukamel, S.; Tretiak, S.; Wagersreiter, T.; Chernyak, V. *Science* **1997**, *277*, 781.

(50) Monshouwer, R.; Abrahamsson, M.; van Mourik, F.; van Grondelle, R. *J. Phys. Chem. B* **1997**, *101*, 7241.

(51) Knoester, J. *J. Lumin.* **1992**, *53*, 101.